

A study of phase separation process with elastic constrains by Monte Carlo method combined with static variational method

H. Ikeda^a and H. Matsuda^b

^aDepartment of Mechanical Engineering, Kagoshima National College of Technology, Hayato-cho, Kagoshima 899-51, Japan

^bEmeritus Professor of Kyushu Institute of Technology, Kitakyushu City, Fukuoka 804, Japan*

We have simulated a phase separation process considering elastic constrain in a substitutional bcc binary alloy by using the Monte Carlo method combined with the static variational method. We have used the Johnson type potentials for the constituents. An isotropic or a little anisotropic structure is generated in the alloy of which elastic constants of the second phase are harder or softer than those of the matrix, and an anisotropic structure is produced in the alloy with the same elastic constants as those of the matrix. The formation of anisotropic structure is not resulted from the growth to the lowest and stable shape of second phase in energy, but from the dynamical process of phase decomposition associated with nonlinear many body effect.

1. INTRODUCTION

It is well known that an elastic constrain influences a phase stability and a shape of the second phase (precipitate) during a phase separation process. Many workers [1-10] have studied the process considering the stable geometric shape of second phase and the elastic effects. However, few three-dimensional discrete model with nonlinear many body effects have been investigated on the dynamical process of phase separation of second phase in elastically anisotropic crystal. We then simulate the phase separation processes by the Monte Carlo method combined with the static variational method using some pairwise interaction potentials between the constituents by constructing a bcc substitutional alloy with elastic anisotropy.

2. SIMULATION METHOD AND MODEL

2.1. Simulation Method

We describe only a short essential features,

as a detailed description of the method is already reported [11]. All lattice sites are occupied randomly with the solute atoms and the vacancies according to the compositions. One of the vacancies is then selected by a random number (R). A vector sum of forces acting to every atom occupying within the 11th nearest neighbor sites from the vacancy is computed by taking a gradient of the pair potential, and then each atom is displaced infinitesimally toward the direction of the force. This variational procedure [12] is iterated until the total interaction energies between the atoms reach to the minimum value (E_i). We adopt one of the nearest neighbor sites of a vacancy for the vacancy jump by use of R , and repeat the same iteration until obtain the minimum value (E_j) of the total energies. We therefore calculate the difference between the total energies before and after the vacancy jump, $\Delta E = E_j - E_i$. If $\Delta E \leq 0$, we make the vacancy migration to the site, and if $\Delta E > 0$, we calculate the transition probability, $P_{ij} = \exp(-\Delta E/k_B T)$ (k_B : the Boltzmann constant, T

*Present address: Kurume Institute of Technology, Kurume City, Fukuoka 830, Japan

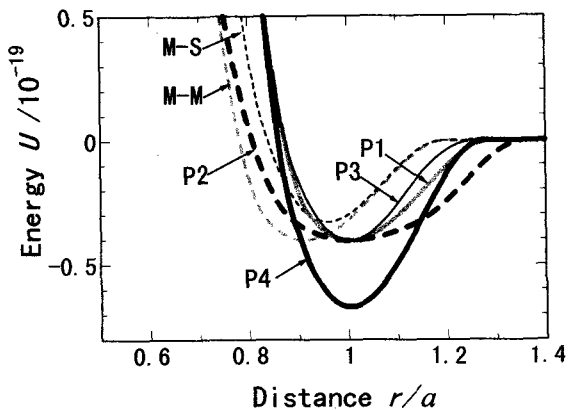


Figure 1. Potential curves used in the present simulations.

: the absolute temperature). Then, if $R \leq R_0$, we make the vacancy jump, otherwise do not. In either case, we take the resultant state as a new state of the crystal and repeat the procedure. We define the number of the procedures as the parameter of time (t) in the present simulations.

2.2. Simulation model

We set following conditions for the simulation; the total number of lattice sites (N): 27000, the vacancy concentration (C_v): 1.85×10^{-3} , the solute atom concentration (C_s): 0.2, the aging temperature (T): 1000 K. A periodic boundary condition is assigned to the crystal. The potential curves used in the present simulation are shown in Figure 1. The curve M-M represents the potential between solvent atoms (matrix) obtained by Johnson [13] for α -iron. The curve M-S also represents the potential between a solvent atom and a solute atom. We have assumed four kinds of

Table 1

Elastic constant ratios of solute atoms (subscript S) to the matrix (=P1) (subscript M) obtained by potential curves of P1, P2, P3 and P4.

	P2	P3	P4
$(C_{11} - C_{12})_S / (C_{11} - C_{12})_M$	0.320	1.20	1.44
$(C_{44})_S / (C_{44})_M$	0.369	1.38	1.66

potential curves between solute atoms (P1, P2, P3, P4) as depicted in Figure 1.

The elastic constants for the potential curves are obtained according to the equations employed by Johnson [13]. The elastic constants of second phase for P1 are equal to those of the matrix, because the curve P1 is obtained by shifting the M-M so that a radius of the solute atom for P1 is 10% larger than that of the matrix. These elastic constant ratios of P2, P3 and P4 to the matrix are listed in Table 1. The second phase for P2 is elastically softer than the matrix, and those for P3 and P4 are harder than the matrix.

3. RESULTS

In the case of the softer second phase than the matrix (P2), the solute atoms formed a site percolation cluster [14]. On the other hand, many isolated clusters are generated for the second phase equal to or harder than the matrix (P1, P3, P4).

We have studied phase separation processes by means of structure function that is a Fourier transform of spatial distribution of solute atoms. According to the results of our analysis by the structure functions, the alloy of which the second phase is elastically equal to the matrix shows a notable anisotropic structure (P1), and a little anisotropic or an isotropic structure is formed in the alloy with the softer or harder second phase than the matrix (P2, P3, P4).

4. DISCUSSION

While the shape of second phase is influenced by many factors, it is considered generally that the harder second phase produces the anisotropic structure more appreciably.

The isotropic phase separation is, however, observed in the alloy with the hardest second phase (P4) in the present simulations. It is considered that as the minimum of potential curve for P4 is lower than any other potentials as illustrated in Figure 1, the interfacial energy overcomes other energies such as the elastic

Table 2

Total energies (E) of atomic configurations computed by the potentials P1, P2, P3 and P4. The underlined values are obtained by using original potentials for respective configurations.

atomic configuration	$E / 10^{-15}$			
	P1	P2	P3	P4
(a) $t=1.2 \times 10^7$	<u>-5.80</u>	-5.88	-5.77	-6.05
(b) $t=2.5 \times 10^6$	-5.75	<u>-6.17</u>	-5.72	-6.13
(c) $t=1.18 \times 10^7$	-5.81	-5.90	<u>-5.78</u>	-6.06
(d) $t=1.321 \times 10^7$	-5.84	-5.95	-5.80	<u>-6.14</u>

energy that effects the anisotropy of the structure in the alloy. The alloy for P4, therefore, generates the isotropic structure.

The curves of P1, P2 and P3 have the same value and position of the minimum, but their shapes are different. Consequently, it is expected that the alloy for P3 exhibits more anisotropic structure than those for P1 and P2, because the second phase of alloy for P3 is elastically harder than the others. The results of simulations, however, show that the anisotropy of the alloy for P3 is not so definite as those for P1. Then, we carried out following calculation to investigate the results. We have applied all potentials (P1, P2, P3, P4) to each configuration of alloy aged for long time to obtain the total energy of each alloy. We summarize these values in Table 2. The underlined values listed in (a), (b), (c) and (d) of the table represent the total energies of the alloys obtained by use of the respective original potentials. The lowest energy in Table 2 is the atomic configuration of alloy by P4 except (b) by P2, this may be caused by the lowest minimum value of the curve P4 in all potential curves. It should be noted that the lowest energy in the atomic configurations is not the atomic configuration produced by original potential P1 (a) but the one by P4 (d), as well as the case of P3 (d).

In order to make clear the reason, we compute changes in energies associated with the formation of cluster containing three solute atoms shown in Figure 2 by using potentials of P1, P2, P3 and P4. In Figure 2, the circles denote the solute atoms, and the numbers

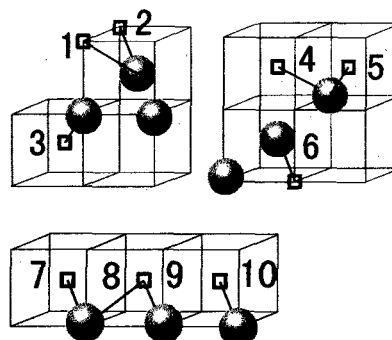


Figure 2. Migration paths for forming a cluster by exchange of a vacancy (a square) and a solute atom (a circle).

Table 3

Changes in total energy (ΔE) of crystals containing 3 solute atoms and one vacancy in forming a cluster via various migration paths as illustrated in Fig.2.

path No.	$\Delta E / 10^{-20} J$			
	P1	P2	P3	P4
1	4.73	1.74	5.64	3.56
2	2.01	-0.133	2.73	-2.24
3	-1.22	-2.53	-0.602	-5.57
4	5.72	1.9	6.36	6.84
5	2.81	-0.552	3.52	1.55
6	5.93	1.95	6.82	5.07
7	-2.49	-2.50	-2.52	-5.18
8	-3.85	-2.02	-4.29	-4.69
9	-6.48	-4.69	-6.88	-9.89
10	-3.85	-2.02	-4.29	-4.69

represent some paths for formation of a cluster after exchanging the vacancy site drawn as square. The changes in total energies are listed in Table 3. The positive value of ΔE means an increase of energy associated with the formation of the cluster. The results for the alloy having three solute atoms and one vacancy are listed in Table 3. In changes of ΔE from No.1 to No.3,

Table 4

Changes in total energy (ΔE) of crystals containing 5403 solute atoms and 51 vacancies in forming a cluster via various migration paths as illustrated in Fig.2. Each value is an average of 5000 configurations.

path	$\Delta E / 10^{-20} \text{J}$			
No.	P1	P2	P3	P4
1	5.46	0.833	4.92	4.17
2	1.97	-0.450	2.11	-1.50
3	-0.757	-1.89	-0.724	-4.48
4	6.91	0.719	5.85	8.01
5	3.58	-0.516	2.78	2.30
6	6.81	1.04	6.01	5.60
7	-2.47	-2.05	-2.29	-4.52
8	-3.92	-1.22	-3.65	-4.43
9	-6.33	-3.06	-6.09	-9.01
10	-4.13	-1.38	-3.80	-4.51

each of No.2 and No.3 of P4 has the smallest and the negative value. This result agrees with the formation of isotropic structure in the alloy for P4. The values of ΔE from No.4 to No.6 are positive for all potentials, except for No.5 of P2. This indicates the difficulty of forming clusters aligned along the $\langle 111 \rangle$ direction. The result that the smallest value of ΔE is obtained for No.4, No.5 and No.6 of P2 explains the growth of site percolation cluster, in which the solute atoms link each other by the first neighbor site or the $\langle 111 \rangle$ direction. All the values of ΔE from No.7 to No.10 are negative. Evidently, the cluster can grow easily along the $\langle 100 \rangle$ direction. Since the value of ΔE from No.1 to No.6 by P1 are less than that by P3, the isotropic cluster can grow more easily by the potential P1 than that by P3. This contradicts to the results of the simulations, and furthermore the tendencies to form clusters along the $\langle 100 \rangle$ direction is not consistent with the results, as all values from No.7 to No.10 of P3 are less than those of P1. We have, therefore, adopted the same atomic configurations of alloys containing a number of solute atoms and vacancies as those used in the

simulations. These results are listed in Table 4, where each value is averaged over 5000 configurations. These values are in consistent with those of the simulations.

5. CONCLUSION

The interaction between the constituents in the formation process of clusters generates an anisotropic growth of cluster. As a result, a lower migration path for atoms brings out the anisotropic arrangement for harder second phase than the matrix. We have then confirmed that the contribution to growth of anisotropic cluster is not from the stable shape in respect to energy but the dynamical process of phase separation.

REFERENCES

1. W. C. Johnson, *Acta Metall.*, 32 (1984) 465.
2. W. C. Johnson and J. W. Cahn, *Acta Metall.*, 32 (1984) 1925.
3. T. Miyazaki, K. Seki, M. Doi and T. Kozakai, *Mater. Sci. Eng.*, 77 (1986) 125.
4. P. W. Voorhees and W. C. Johnson, *Phys. Rev. Lett.*, 61 (1988) 2225.
5. K. Kawasaki and Y. Enomoto, *Physica*, 150A (1988) 463.
6. J. K. Lee, *Metall. Trans.*, 22A (1991) 1197.
7. A. Onuki and H. Nishimori, *J. Phys. Soc. Jpn.*, 60 (1991) 1.
8. A. Takeuchi, T. Koyama and T. Miyazaki, *J. Japan Inst. Metals* 57 (1993) 492.
9. Y. Wang, L. Q. Chen and A. G. Khachaturyan, *Acta Metall.*, 41 (1993) 279.
10. Y. Wang and A. G. Khachaturyan, *Acta Metall.*, 43 (1995) 1837.
11. H. Ikeda and H. Matsuda, *J. Japan Inst. Metals*, 54 (1990) 1171; *Mater. Trans.*, JIM, 33 (1992) 466.
12. R. A. Johnson and E. Brown, *Phys. Rev.*, 127 (1962) 446.
13. R. A. Johnson, *Phys. Rev.*, 134 (1964) A1329.
14. H. Ikeda and H. Matsuda, *J. Japan Inst. Metals*, 56 (1992) 1378; *Mater. Trans.*, JIM, 34 (1993) 651.